Relation of Coronary Microvascular Dysfunction in Hypertrophic Cardiomyopathy to Contractile Dysfunction Independent from Myocardial Injury

Stefan A.J. Timmer, BSc[a], Tjeerd Germans, MD[a], Marco J.W. Götte, MD[a], Iris K. Rüssel, PhD[a], Mark Lubberink, PhD[b], Jurrien M. ten Berg, MD[c], Folkert J. ten Cate, MD[d], Adriaan A. Lammertsma, PhD[b], Paul Knaapen, MD[a,*], and Albert C. van Rossum, MD[a]

We studied the spatial relations among hyperemic myocardial blood flow (hMBF), contractile function, and morphologic tissue alterations in 19 patients with hypertrophic cardiomyopathy (HC). All patients were studied with oxygen-15 water positron emission tomography during rest and adenosine administration to assess myocardial perfusion. Cardiovascular magnetic resonance was performed to derive delayed contrast-enhanced images and to calculate contractile function (E_{cc}) with tissue tagging. Eleven healthy subjects underwent similar positron emission tomographic and cardiovascular magnetic resonance scanning protocols and served as a control group. In the HC group, hMBF averaged 2.46 ± 0.91 ml/min/g and mean E_{cc} was −14.7 ± 3.4%, which were decreased compared to the control group (3.97 ± 1.48 ml/min/g and −17.7 ± 3.2%, respectively, $p < 0.001$ for the 2 comparisons). Delayed contrast enhancement (DCE) was present only in patients with HC, averaging 6.2 ± 10.3% of left ventricular mass. In the HC group, E_{cc} and DCE in the septum (−13.7 ± 3.6% and 10.2 ± 13.6%) significantly differed from the lateral wall (−16.0 ± 2.8% and 2.4 ± 5.9%, $p < 0.001$ for the 2 comparisons). In general, hMBF and E_{cc} were decreased in segments displaying DCE compared to nonenhanced segments ($p < 0.001$ for the comparisons). In the HC group, univariate analysis revealed relations of hMBF to E_{cc} ($r = -0.45$, $p < 0.001$) and DCE ($r = -0.31$, $p < 0.001$). Multivariate analysis revealed that E_{cc} was independently related to hMBF (beta −0.37, $p < 0.001$) and DCE (beta 0.28, $p < 0.001$). In conclusion, in HC hMBF is impaired and related to contractile function independent from presence of DCE. When present, DCE reflected a progressed disease state as characterized by an increased perfusion deficit and contractile dysfunction. **(Am J Cardiol 2011;107:1522–1528)**

Microvascular dysfunction is a common feature in patients with hypertrophic cardiomyopathy (HC), despite angiographically normal coronary artery anatomy.[1] Consequently, hyperemic myocardial blood flow (hMBF) is hampered.[2–8] It has been postulated that microvascular dysfunction predisposes to myocardial ischemia, resulting in contractile dysfunction and scar formation.[9] Indeed, hMBF measured with first-pass cardiovascular magnetic resonance imaging or nitrogen-13 ammonia positron emission tomography has been related to wall thickening and delayed contrast-enhanced cardiovascular magnetic resonance imaging.[5,7] However, scar tissue affects the kinetics of gadolinium and uptake of nitrogen-13 ammonia,[10,11] and thus estimates of perfusion. In addition, systolic wall thickening has limited accuracy as a marker of contractile function in the presence of left ventricular (LV) hypertrophy. Oxygen-15–labeled water positron emission tomography, however, determines perfusion in perfusable tissue only, excluding scar tissue from its MBF estimates. In addition, cardiovascular magnetic resonance tissue tagging yields data on myocardial systolic deformation independent from wall thickness, thus serving as a more reliable index of contraction.[12] Therefore, the present study was conducted to investigate interrelations in hMBF, regional contractile function, and myocardial injury using oxygen-15–labeled water positron emission tomographic versus cardiovascular magnetic resonance tissue tagging and delayed contrast enhancement (DCE).

Methods

Nineteen patients with symptomatic HC were enrolled in the study. HC was diagnosed according to presence of LV septal hypertrophy on 2-dimensional echocardiography (maximal wall thickness >15 mm in adults or >13 mm in relatives of a patient with HC) in the absence of any other systemic or cardiac disease.[13] All patients exhibited asymmetrical LV hypertrophy at the interventricular septum. All patients underwent coronary angiography to exclude presence of coronary artery disease. Use of medication at time of enrollment was not

Departments of [a]Cardiology and [b]Nuclear Medicine and PET Research, VU University Medical Center, Amsterdam, The Netherlands; [c]Department of Cardiology, St. Antonius Hospital, Nieuwegein, The Netherlands; [d]Department of Cardiology, Thoraxcenter Erasmus Medical Center, Rotterdam, The Netherlands. Manuscript received November 30, 2010; revised manuscript received and accepted January 11, 2011.

*Corresponding author: Tel: 31-20-444-2244; fax: 31-20-444-2446.
E-mail address: p.knaapen@vumc.nl (P. Knaapen).

0002-9149/11/$ – see front matter
doi:10.1016/j.amjcard.2011.01.029

discontinued during the study. Eleven healthy volunteers with normal electrocardiogram, normal physical examination, and without a relevant medical history were included as a control group. The study protocol was approved by the medical ethics review committee of the VU University Medical Center, Amsterdam, The Netherlands.

All positron emission tomographic scans were acquired using an ECAT EXACT HR+ scanner (Siemens/CTI, Knoxville, Tennessee) in 2-dimensional mode. All patients were monitored with single-lead electrocardiography and blood pressure and heart rate were recorded at regular intervals during positron emission tomographic studies. A transmission scan was performed using 3 rotating rod sources filled with gallium-68/germanium-68 solution. Subsequently, oxygen-15–labeled water 1,100 MBq dissolved in a 5-ml saline solution was injected intravenously, followed by a 40-ml saline solution flush at a rate of 4 ml/s. A dynamic emission scan was acquired, consisting of 40 frames with variable frame length for a total time of 10 minutes (12 × 5, 12 × 10, 6 × 20, and 10 × 30 seconds). After the study at rest, MBF was determined during hyperemia by infusion of adenosine at a rate of 140 μg/kg of body weight per minute. Emission data were corrected for physical decay of oxygen-15, dead time, scatter, randoms, and photon attenuation. Cardiovascular magnetic resonance studies were performed in a 1.5-T whole body scanner (Magnetom Sonata, Siemens, Erlangen, Germany) using a 6-channel phased-array body coil. After survey scans, a retro-triggered balanced steady-state free precession gradient-echocardiographic sequence was used for cine imaging. Image parameters were slice thickness 5 mm, slice gap 5 mm, temporal resolution <50 ms, repetition time 3.2 ms, echocardiographic time 1.54 ms, flip angle 60°, and typical image resolution 1.3 × 1.6 mm. Number of phases within the cardiac cycle was set at 20. Four-, 3-, and 2-chamber view cine images were obtained.[14] Then, a stack of 10 to 12 short-axis slices covering the left ventricle was used for assessing LV volumes, mass, and ejection fraction. The method of planning image acquisition for LV coverage has been described previously.[15] Cine images were acquired during 1 breath-hold in mild expiration. Cine imaging with myocardial tagging was applied to create noninvasive markers (tags) within the myocardium for calculation of strain.[16] Five short-axis tagged images with complementary spatial modulation of magnetization tagging for improved strain calculations were acquired as previously described.[17] Delayed contrast-enhanced images were acquired 10 to 15 minutes after intravenous administration of gadolinium 0.2 mmol/kg using a 2-dimensional segmented inversion-recovery prepared gradient-echocardiographic sequence. Inversion-recovery time was 250 to 300 ms.

Data were transferred to a SUN workstation (SUN Microsystems Inc., Knoxville, Tennessee) and analyzed using Siemens/CTI software and an additional tracer kinetic analysis software developed in MATLAB (Mathworks, Natick, Masssachusetts). Reconstruction of oxygen-15–labeled water emission sinograms was performed using filtered backprojection with a Hanning filter at 0.5 of Nyquist frequency, resulting in a transaxial spatial resolution of ≈7 mm full width at 1/2 maximum. Regions of interest were defined manually on oxygen-15–labeled water short-axis summed-uptake images at basal, midventricular, and apical levels of the left ventricle according to a 12-segment model as described previously in detail.[10] This set of regions of interest was projected onto dynamic oxygen-15–labeled water images to generate time–activity curves. Additional regions of interest were defined in the left atrial and right ventricular blood pools. This latter set of regions of interest was projected onto the dynamic oxygen-15–labeled water images to generate time–activity curves of intravascular activity. These time–activity curves were used as image-derived input functions and for use in spillover correction of myocardial tissue time–activity curves. Using a standard single tissue compartment model, MBF (milliliters per minute per gram of perfusable tissue) was determined for all myocardial oxygen-15–labeled water time–activity curves.[18] Average MBF was calculated by grouping all regions of interest, whereas regional blood flows were calculated by grouping specific regions of interest. Corrections were made for LV and right ventricular spillover effects using the method described by Hermansen et al.[19] In addition, coronary microvascular resistance at rest was calculated by dividing mean arterial pressure by MBF, whereas minimal coronary microvascular resistance was derived in similar fashion only during hyperemic conditions.[20] LV volume analysis was performed by manually drawing epicardial and endocardial contours on all end-diastolic and end-systolic LV short-axis images. Global LV function parameters including end-diastolic volume, end-systolic vol-

Table 1
Baseline characteristics

Characteristic	HC (n = 19)	Control (n = 11)	p Value
Men/women	11/8	7/4	0.77
Age (years)	55 ± 14	53 ± 3	0.86
Body surface area (m^2)	2.1 ± 0.2	2.0 ± 0.2	0.72
Left ventricular mass (g)	178 ± 58	99 ± 21	<0.001
Left ventricular end-diastolic volume (ml)	191 ± 33	179 ± 33	0.80
Left ventricular end-systolic volume (ml)	76 ± 20	73 ± 21	0.72
Left ventricular ejection fraction (%)	59 ± 8	61 ± 5	0.98
Left ventricular outflow tract obstruction (>30 mm Hg)	5 (26%)	0	<0.001
NH_2-terminal pro–brain natriuretic peptide (ng/L)	535 ± 536	61 ± 53	<0.001

Table 2
Medication specifications of hypertrophic cardiomyopathic patients

Medication	Patients (%)
None	4 (21%)
Metoprolol 100 mg	4 (21%)
Metoprolol 50 mg	2 (11%)
Bisoprolol 2.5 mg	2 (11%)
Metoprolol 50 mg, diltiazem 300 mg	2 (11%)
Bisoprolol 2.5 mg, verapamil 180 mg	2 (11%)
Metoprolol 100 mg, verapamil 80 mg	1 (5%)
Verapamil 240 mg	1 (5%)
Diltiazem 200 mg	1 (5%)

Table 3
Hemodynamic parameters during positron emission tomography

	At Rest			Hyperemia		
	HC	Control	p Value	HC	Control	p Value
Systolic blood pressure (mm Hg)	130 ± 25	124 ± 16	0.48	112 ± 19	122 ± 12	0.13
Diastolic blood pressure (mm Hg)	75 ± 9	73 ± 8	0.55	64 ± 8	65 ± 8	0.74
Mean arterial pressure (mm Hg)	94 ± 13	90 ± 10	0.52	80 ± 10	84 ± 8	0.27
Heart rate (beats/min)	61 ± 9	66 ± 11	0.19	87 ± 14	95 ± 15	0.15

Table 4
Regional positron emission tomographic and cardiovascular magnetic resonance data for hypertrophic cardiomyopathic patients (n = 19) and controls (n = 11)

Region	MBF (ml/min/g)		hMBF (ml/min/g)		E_{cc} (%)		DCE (%)	
	HC	Control	HC	Control	HC	Control	HC	Control
Anterior	1.00 ± 0.22	1.18 ± 0.32	2.36 ± 1.01	4.40 ± 1.37	−14.3 ± 3.3	−16.9 ± 2.9	7.1 ± 10.6	0
Lateral	1.02 ± 0.27*†	1.18 ± 0.35	2.54 ± 0.99	3.73 ± 1.30	−16.0 ± 2.8	−18.8 ± 3.2	2.4 ± 5.9	0
Inferior	0.86 ± 0.24	0.96 ± 0.30	2.43 ± 1.23	4.37 ± 2.02	−14.5 ± 3.4	−17.5 ± 3.4	4.5 ± 5.5*	0
Septal	0.90 ± 0.24	1.05 ± 0.40	2.34 ± 1.02	3.80 ± 1.35	−13.7 ± 3.6‡	−17.1 ± 3.2	10.2 ± 13.6‡	0
Average	0.96 ± 0.21	1.09 ± 0.36	2.46 ± 0.91	3.97 ± 1.48	−14.7 ± 3.4	−17.7 ± 3.2	6.2 ± 10.3	0

In the hypertrophic cardiomyopathy group, p values (as determined by analysis of variance) for myocardial blood flow, hyperemic myocardial blood flow, contractile function, and delayed contrast enhancement were 0.002, 0.70, <0.001, and <0.001, respectively. In the control group, p values (as determined by analysis of variance) for myocardial blood flow, hyperemic myocardial blood flow, contractile function, and delayed contrast enhancement were 0.08, 0.15, 0.05, and 1.

* $p < 0.05$ versus septal.
† $p < 0.01$ versus inferior.
‡ $p < 0.001$ versus lateral.

ume, ejection fraction, and myocardial mass were then derived from cine images using MASS software (MEDIS, Leiden, The Netherlands). Tagging images were used to generate circumferential strain curves for each myocardial segment. Subsequently, maximum contractile function (E_{cc}) was derived for each segment from the strain curves.[17] Similar segmentation for average and regional analyses of E_{cc} was used as described for positron emission tomographic data. Because circumferential shortening is determined by shortening of myofibers, E_{cc} is expressed as a negative value. Each myocardial segment was evaluated for presence of hyperenhancement, which was defined as an area of signal enhancement >5 SD of the signal of nonenhanced myocardium. Extent of DCE was expressed as percent total myocardial tissue area studied. Similar segmentation for average and regional analyses of myocardial hyperenhancement was used as described for positron emission tomographic data.

Results are presented as mean ± SD. For comparison of 2 datasets, unpaired Student's *t* test was used. For comparison of multiple datasets, 1-way analysis of variance was applied with post hoc Bonferroni adjustment for inequality. Correlations between variables were evaluated with univariate and multivariate analyses. All tests were performed 2-sided and a p value <0.05 was considered statistically significant.

Results

Baseline characteristics of the HC and control study populations are presented in Table 1. All patients HC except 4, in whom side effects were considered intolerable, used β-receptor blockers and/or calcium channel blockers, the subtypes and dosages of which are specified in Table 2. Hemodynamic parameters obtained during at-rest and hyperemic positron emission tomographic studies are listed in Table 3.

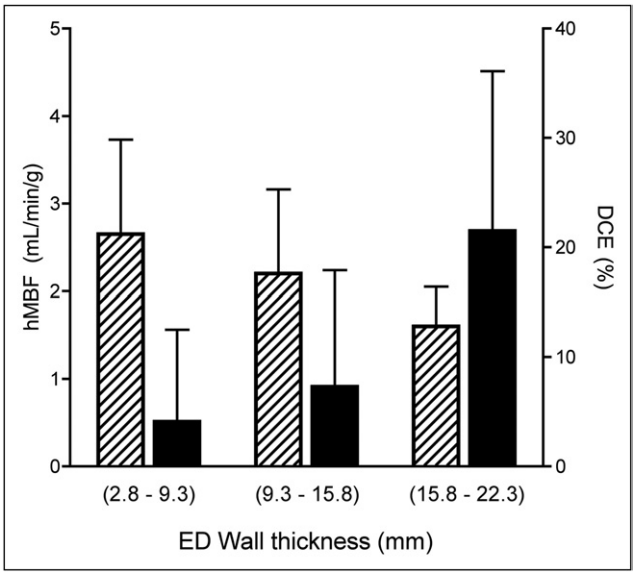

Figure 1. Bar charts depict hyperemic myocardial blood flow values *(hatched bars)* and extent of delayed contrast enhancement *(black bars)* in relation to end-diastolic (ED) wall thickness. Analysis of variance was significant for the 2 trends ($p < 0.001$).

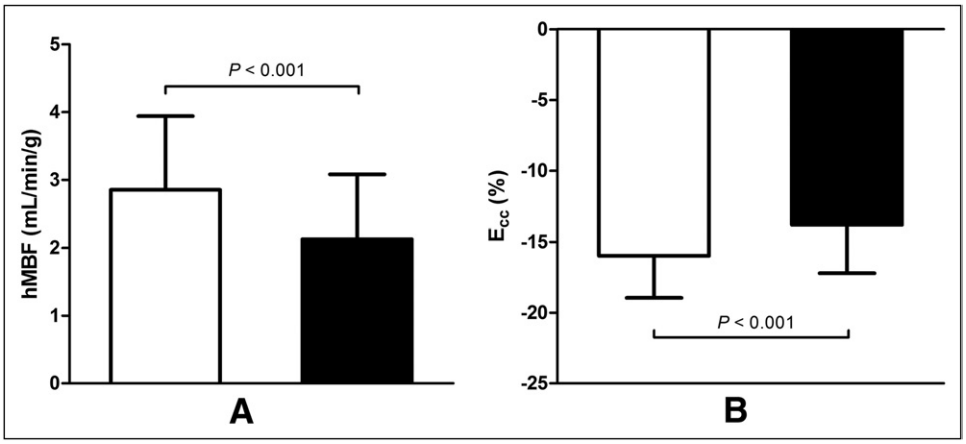

Figure 2. Bar charts depict hyperemic myocardial blood flow values for all hypertrophic cardiomyopathic segments *(A)* without *(white bars)* and with *(black bars)* delayed contrast enhancement and *(B)* varying degrees of contractile function categorized as normal (>18.0%), moderately (18.0% to 11.5%), and severely (<11.5%) impaired.

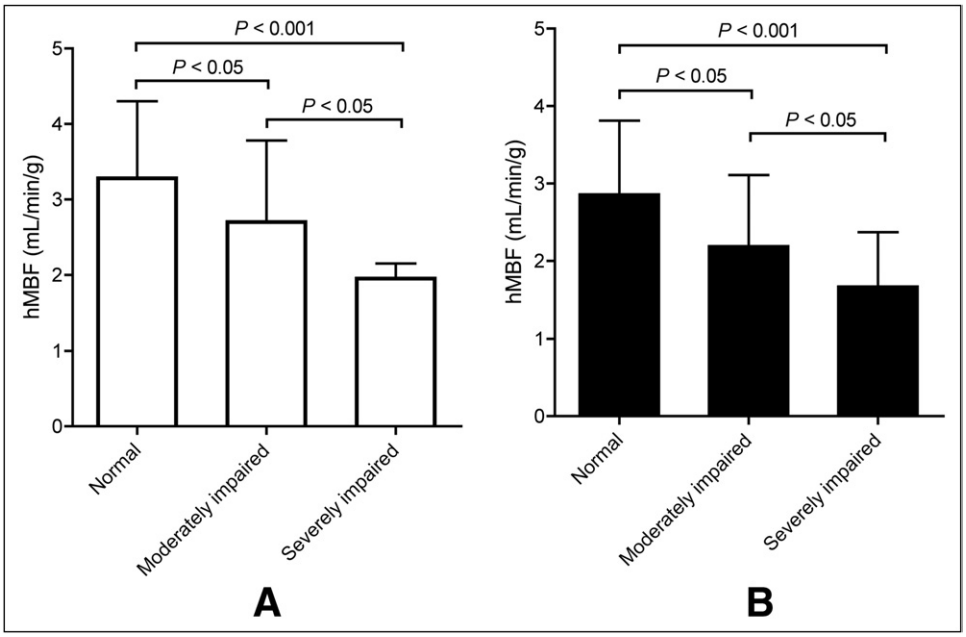

Figure 3. Bar chart demonstrates that hyperemic myocardial blood flow *(A)* and contractile function *(B)* are significantly impaired in regions that display delayed contrast enhancement *(black bars)* compared to nonenhanced segments *(white bars)*.

Table 4 presents regional at-rest and hMBF, E_{cc}, and DCE for the 2 study groups. In total 228 segments were analyzed in the HC group and 132 in the control group (12 segments per subject). In the HC group, MBF at rest averaged 0.96 ± 0.21 ml/min/g and was slightly lower compared to the control group (1.09 ± 0.36 ml/min/g, p = 0.10). MBF was significantly decreased in the hypertrophied septum and inferior wall compared to the lateral wall (p <0.01 and p <0.05, respectively). Hyperemic MBF in the HC group averaged 2.46 ± 0.91 ml/min/g, which was significantly lower compared to the control group (3.97 ± 1.48 ml/min/g, p <0.001). In the 2 study groups, hMBF was distributed homogenously across all regions. E_{cc} in the HC group averaged −14.7 ± 3.4%, which was significantly lower compared to controls (−17.7 ± 3.2%, p <0.001). In addition, E_{cc} was distributed more heterogenously in HC, with significant impairment of E_{cc} in the hypertrophied septum compared to the lateral wall (p <0.001). On average, 6 ± 10% of the myocardium displayed DCE in HC, predominantly localized in the basal anteroseptal region at the junction with the right ventricular free wall (14 ± 12%). Mean end-diastolic wall thickness of the hypertrophied septum was 16.3 ± 2.8 mm. Analysis of all myocardial HC segments revealed that hMBF decreased in proportion to the increase in end-diastolic wall thickness (p <0.001, analysis of variance; Figure 1). In contrast, extent of DCE increased in proportion to the increase in end-diastolic wall thickness (p <0.001, analysis of variance). During conditions at rest, coronary microvascular resistance was 102 ± 22 mm Hg/ml/min in the HC group, which was not significantly different from the control group (86 ± 19 mm Hg/ml/min, p = 0.07). Coronary microvascular resistance during hyperemic conditions, however, was significantly

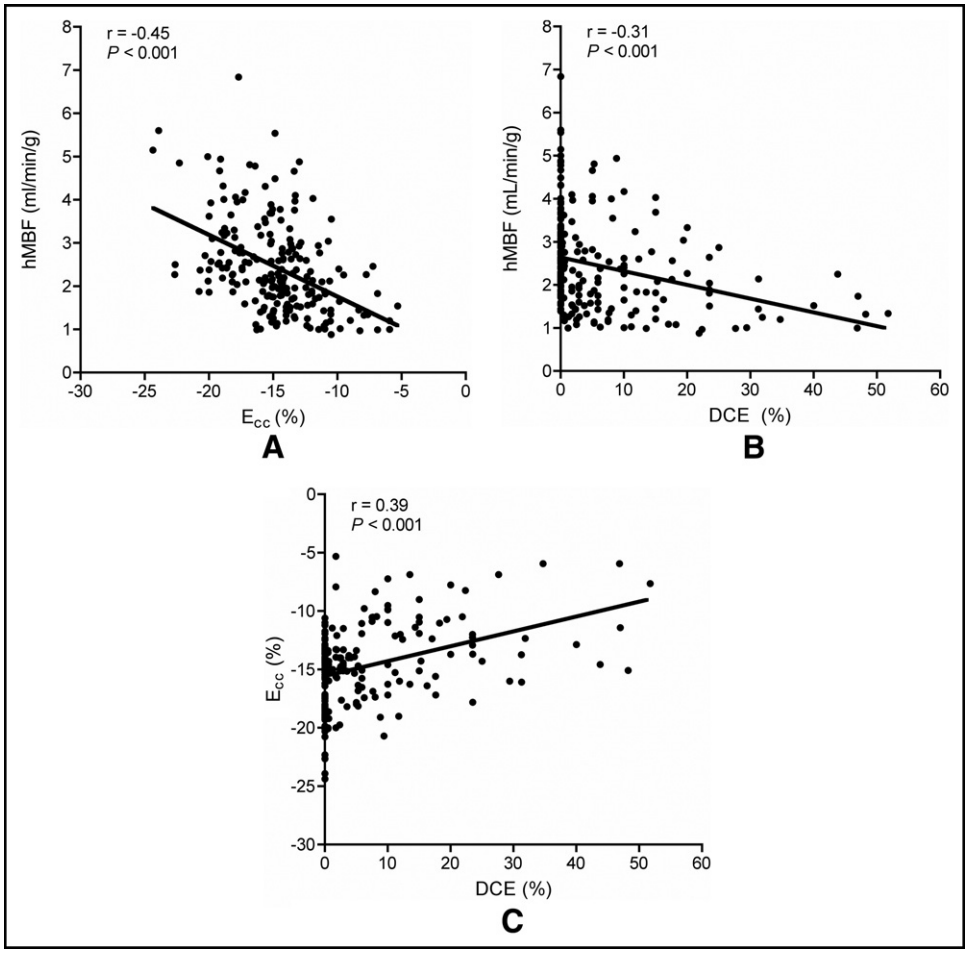

Figure 4. Scatterplots demonstrate linear relations in hypertrophic cardiomyopathy between *(A)* hyperemic myocardial blood flow and contractile function, *(B)* hyperemic myocardial blood flow and delayed contrast enhancement, and *(C)* contractile function and delayed contrast enhancement.

higher compared to controls (37 ± 15 vs 22 ± 6 mm Hg/ml/min, p = 0.004).

Figure 2 demonstrates that hMBF and E_{cc} were significantly dcreased in segments displaying DCE (n = 120) compared to segments without DCE (n = 108, p <0.001 for the 2 comparisons) in the HC group. In myocardial HC segments without DCE, hMBF was significantly affected by extent of contractile dysfunction (expressed as E_{cc}, from normal to severely impaired, p <0.001, analysis of variance; Figure 3). A similar relation between hMBF and E_{cc} was found when only segments with DCE were analyzed (p <0.001, analysis of variance; Figure 3). Nonenhanced segments exhibiting severely impaired E_{cc} (n = 5) were exceptional as were hyperenhanced segments with normal E_{cc} (n = 8), with an average DCE extent of only 1 ± 2%. In the HC group, univariate analysis demonstrated that regional hMBF was inversely related to E_{cc} (r = −0.45, p <0.001) and extent of DCE (r = −0.31, p <0.001). A linear relation was also observed between extent of DCE and E_{cc} (r = 0.39, p <0.001). Multivariate analysis revealed that E_{cc} was independently related to hMBF (beta −0.37, p <0.001) and DCE (beta 0.28, p <0.001). Figure 4 shows these relations in scatter plots.

Discussion

In patients with HC, coronary microvascular dysfunction results in blunted hMBF, especially in areas with pronounced hypertrophy, typically the interventricular septum.[5,6] Similarly, patients with LV hypertrophy from hypertension or aortic stenosis also have decreased hMBF,[21,22] implying that pathologic hypertrophy itself substantially impedes myocardial perfusion, presumably because of a relative decrease in capillary density. Interestingly, hMBF was homogenously decreased across the entire myocardium. Hence, microvascular dysfunction is not solely confined to the septum but appears as a widespread phenomenon also affecting nonhypertrophied areas.[2,8] These observations suggest diffuse impairment of microvascular function, which is supported by histologic findings of intramural coronary artery remodeling throughout the LV myocardium.[23] In addition, increased coronary microvascular resistance caused by augmented extravascular compressive forces from LV outflow tract obstruction also have independently been related to microvascular dysfunction.[13,24]

MBF at rest was significantly decreased in hypertrophied septal regions compared to the lateral free wall and has been linked to interventricular localization of DCE.[11,25] Corre-

spondingly, extent of DCE in the present HC study group was significantly largest in the septum, principally affecting the anteroseptal segment. Cardiovascular magnetic resonance tagging data revealed significant impairment of contractile function of the hypertrophied septum.[25,26] Interestingly, contractile function of the nonhypertrophied lateral wall was also decreased, albeit to a much lesser degree than the septum. The main finding of this study was that regional hMBF in HC was significantly correlated to contractile function irrespective of presence of DCE. Furthermore, extent of DCE was independently and inversely related to contractile function.

A blunted perfusion reserve in HC has been associated with loss of contractile function in other cross-sectional reports.[3,5,7,8] In this study, increase of MBF after adenosine infusion, i.e., coronary vasodilatory reserve, was significantly blunted. Consequently, microvascular dysfunction in HC predisposes to myocardial ischemia and may result in ischemic injury with loss of contractile function and secondary replacement fibrosis.[7,8] Correspondingly, the present data revealed that hMBF decreased in proportion to extent of contractile dysfunction in the absence and presence of DCE. This hypothesis was recently corroborated by a follow-up study conducted by Olivotto et al[4] who demonstrated that patients with HC and a severe perfusion reserve deficit are at increased risk for developing contractile dysfunction during follow-up even in the absence of abnormal contractile function or tissue function at the start of the study. Histologic examination of HC hearts has revealed a disorganized structure of cardiomyocytes in the hypertrophied septum, seemingly leading to decreased contractile function on a macroscopic level with normal oxidative metabolism. Inasmuch as this myofiber disarray is presumably the result of mutations in the abnormal sarcomeric protein, it is at least in part considered an independent process of microvascular capacity.[27] Therefore, presence of myocyte disarray alone could also contribute to significant impairment of contractile function of the hypertrophied septum observed in the present study.

Hyperemic MBF was significantly more decreased in segments displaying DCE compared to nonenhanced segments, which has been documented previously during hyperemic[7] and at-rest myocardial perfusion positron emission tomographic studies.[25] Next to fibrosis, DCE is thought to reflect several other substrates in HC,[28] the interpretation of which is presumably dependent on the stage of the disease process. In the acute or subacute ischemic phase DCE may reflect inflammation, focal edema, and myocyte necrosis, whereas in the long-term phase these hyperenhanced foci are likely to be the gross result of interstitial and replacement fibrosis.[29] The present data also demonstrated decreased hMBF values in the absence of DCE. This suggests that microvascular dysfunction constitutes a primary component of the HC phenotype, with secondary occurrence of ischemic injury and subsequent acute and long-term tissue responses, which are reflected by DCE.[9] Concordant with the latter hypothesis are cross-sectional findings by Sotgia et al[7] who also observed correlations of impaired hMBF with DCE and contractile dysfunction.[7] It has been shown that loss of perfusion reserve in delayed contrast-enhanced negative areas nearby or adjacent to hyperenhanced areas is more pronounced compared to remote segments.[5,7] In our study, DCE also extended to the nonhypertrophied lateral wall, which could be explained by the fact that microvascular dysfunction is not solely confined to areas with hypertrophy, although it does correlate in severity with magnitude of segmental hypertrophy.

In the present study population, nearly every myocardial segment with severe contractile dysfunction also displayed hyperenhancement. Extensive presence of DCE has been associated with significant impairment of contractile function in various other HC investigations.[26,29–31] Histologic examination has confirmed that replacement and interstitial fibrosis are distinctive features of end-stage HC hearts.[23] Accordingly, a contributable role for myocardial fibrosis in impeding systolic function, by mechanically interfering with myocardial shortening, should be considered.[17,25,26] This is underlined by the present significant relation between contractile dysfunction and hyperenhancement regardless of hMBF.

All together these results imply that patients with HC and relatively large perfusion defects are at increased risk of developing contractile dysfunction and myocardial fibrosis, with a concomitant risk of heart failure and potentially lethal arrhythmias in the long term.[4] Hence, early detection of segments with abnormal perfusion may warrant initiation of treatment strategies that could protect the myocardium against repetitive ischemic episodes, e.g., β-blocker therapy,[32] or ameliorate perfusion defects in the presence of significant LV outflow tract obstruction using alcohol septal ablation/surgical myectomy.[6]

A limitation of the present study is the small sample, which could have limited the statistical accuracy of our results. This is especially relevant when aspects of the myocardium are compared on a regional and/or segmental level where absolute differences in and between study groups are small. Furthermore, drug treatment was sustained because of ethical reasons.

Although calcium channel blocker agents exert little effect on at-rest and hyperemic blood flow,[33] β-receptor blockers have been shown to significantly decrease stroke volume and ejection fraction, and therefore their effect on regional contractile function may be substantial.[34] This might have influenced our results and introduced bias compared to the control group.

1. Maron BJ. Hypertrophic cardiomyopathy: a systematic review. *JAMA* 2002;287:1308–1320.
2. Camici P, Chiriatti G, Lorenzoni R, Bellina RC, Gistri R, Italiani G, Parodi O, Salvadori PA, Nista N, Papi L. Coronary vasodilation is impaired in both hypertrophied and nonhypertrophied myocardium of patients with hypertrophic cardiomyopathy: a study with nitrogen-13 ammonia and positron emission tomography. *J Am Coll Cardiol* 1991; 17:879–886.
3. Lorenzoni R, Gistri R, Cecchi F, Olivotto I, Chiriatti G, Elliott P, McKenna WJ, Camici PG. Coronary vasodilator reserve is impaired in patients with hypertrophic cardiomyopathy and left ventricular dysfunction. *Am Heart J* 1998;136:972–981.
4. Olivotto I, Cecchi F, Gistri R, Lorenzoni R, Chiriatti G, Girolami F, Torricelli F, Camici PG. Relevance of coronary microvascular flow impairment to long-term remodeling and systolic dysfunction in hypertrophic cardiomyopathy. *J Am Coll Cardiol* 2006;47:1043–1048.
5. Petersen SE, Jerosch-Herold M, Hudsmith LE, Robson MD, Francis JM, Doll HA, Selvanayagam JB, Neubauer S, Watkins H. Evidence for microvascular dysfunction in hypertrophic cardiomyopathy: new in-

sights from multiparametric magnetic resonance imaging. *Circulation* 2007;115:2418–2425.
6. Soliman OI, Geleijnse ML, Michels M, Dijkmans PA, Nemes A, Van Dalen BM, Vletter WB, Serruys PW, ten Cate FJ. Effect of successful alcohol septal ablation on microvascular function in patients with obstructive hypertrophic cardiomyopathy. *Am J Cardiol* 2008;101: 1321–1327.
7. Sotgia B, Sciagra R, Olivotto I, Casolo G, Rega L, Betti I, Pupi A, Camici PG, Cecchi F. Spatial relationship between coronary microvascular dysfunction and delayed contrast enhancement in patients with hypertrophic cardiomyopathy. *J Nucl Med* 2008;49:1090–1096.
8. Cecchi F, Olivotto I, Gistri R, Lorenzoni R, Chiriatti G, Camici PG. Coronary microvascular dysfunction and prognosis in hypertrophic cardiomyopathy. *N Engl J Med* 2003;349:1027–1035.
9. Maron MS, Olivotto I, Maron BJ, Prasad SK, Cecchi F, Udelson JE, Camici PG. The case for myocardial ischemia in hypertrophic cardiomyopathy. *J Am Coll Cardiol* 2009;54:866–875.
10. Knaapen P, Boellaard R, Götte MJ, Dijkmans PA, van Campen LM, de Cock CC, Luurtsema G, Visser CA, Lammertsma AA, Visser FC. Perfusable tissue index as a potential marker of fibrosis in patients with idiopathic dilated cardiomyopathy. *J Nucl Med* 2004;45:1299–1304.
11. Choudhury L, Mahrholdt H, Wagner A, Choi KM, Elliott MD, Klocke FJ, Bonow RO, Judd RM, Kim RJ. Myocardial scarring in asymptomatic or mildly symptomatic patients with hypertrophic cardiomyopathy. *J Am Coll Cardiol* 2002;40:2156–2164.
12. Dong SJ, MacGregor JH, Crawley AP, McVeigh E, Belenkie I, Smith ER, Tyberg JV, Beyar R. Left ventricular wall thickness and regional systolic function in patients with hypertrophic cardiomyopathy. A three-dimensional tagged magnetic resonance imaging study. *Circulation* 1994;90:1200–1209.
13. Knaapen P, Germans T, Camici PG, Rimoldi OE, ten Cate FJ, ten Berg JM, Dijkmans PA, Boellaard R, van Dockum WG, Gotte MJ, Twisk JW, van Rossum AC, Lammertsma AA, Visser FC. Determinants of coronary microvascular dysfunction in symptomatic hypertrophic cardiomyopathy. *Am J Physiol Heart Circ Physiol* 2008;294:H986–H993.
14. Germans T, Götte MJ, Nijveldt R, Spreeuwenberg MD, Beek AM, Bronzwaer JG, Visser CA, Paulus WJ, van Rossum AC. Effects of aging on left atrioventricular coupling and left ventricular filling assessed using cardiac magnetic resonance imaging in healthy subjects. *Am J Cardiol* 2007;100:122–127.
15. Marcus JT, Götte MJ, DeWaal LK, Stam MR, Van der Geest RJ, Heethaar RM, Van Rossum AC. The influence of through-plane motion on left ventricular volumes measured by magnetic resonance imaging: implications for image acquisition and analysis. *J Cardiovasc Magn Reson* 1999;1:1–6.
16. Götte MJ, Germans T, Rüssel IK, Zwanenburg JJ, Marcus JT, van Rossum AC, van Veldhuisen DJ. Myocardial strain and torsion quantified by cardiovascular magnetic resonance tissue tagging: studies in normal and impaired left ventricular function. *J Am Coll Cardiol* 2006;48:2002–2011.
17. Knaapen P, Götte MJ, Paulus WJ, Zwanenburg JJ, Dijkmans PA, Boellaard R, Marcus JT, Twisk JW, Visser CA, van Rossum AC, Lammertsma AA, Visser FC. Does myocardial fibrosis hinder contractile function and perfusion in idiopathic dilated cardiomyopathy? PET and MR imaging study. *Radiology* 2006;240:380–388.
18. Iida H, Kanno I, Takahashi A, Miura S, Murakami M, Takahashi K, Ono Y, Shishido F, Inugami A, Tomura N. Measurement of absolute myocardial blood flow with H215O and dynamic positron-emission tomography. Strategy for quantification in relation to the partial-volume effect. *Circulation* 1988;78:104–115.
19. Hermansen F, Rosen SD, Fath-Ordoubadi F, Kooner JS, Clark JC, Camici PG, Lammertsma AA. Measurement of myocardial blood flow with oxygen-15 labelled water: comparison of different administration protocols. *Eur J Nucl Med* 1998;25:751–759.
20. Knaapen P, Camici PG, Marques KM, Nijveldt R, Bax JJ, Westerhof N, Götte MJ, Jerosch-Herold M, Schelbert HR, Lammertsma AA, van Rossum AC. Coronary microvascular resistance: methods for its quantification in humans. *Basic Res Cardiol* 2009;104:485–498.
21. Gimelli A, Schneider-Eicke J, Neglia D, Sambuceti G, Giorgetti A, Bigalli G, Parodi G, Pedrinelli R, Parodi O. Homogeneously reduced versus regionally impaired myocardial blood flow in hypertensive patients: two different patterns of myocardial perfusion associated with degree of hypertrophy. *J Am Coll Cardiol* 1998;31:366–373.
22. Rajappan K, Rimoldi OE, Camici PG, Bellenger NG, Pennell DJ, Sheridan DJ. Functional changes in coronary microcirculation after valve replacement in patients with aortic stenosis. *Circulation* 2003; 107:3170–3175.
23. Maron BJ, Wolfson JK, Epstein SE, Roberts WC. Intramural ("small vessel") coronary artery disease in hypertrophic cardiomyopathy. *J Am Coll Cardiol* 1986;8:545–557.
24. Soliman OI, Knaapen P, Geleijnse ML, Dijkmans PA, Anwar AM, Nemes A, Michels M, Vletter WB, Lammertsma AA, ten Cate FJ. Assessment of intravascular and extravascular mechanisms of myocardial perfusion abnormalities in obstructive hypertrophic cardiomyopathy by myocardial contrast echocardiography. *Heart* 2007;93: 1204–1212.
25. Knaapen P, van Dockum WG, Götte MJ, Broeze KA, Kuijer JP, Zwanenburg JJ, Marcus JT, Kok WE, van Rossum AC, Lammertsma AA, Visser FC. Regional heterogeneity of resting perfusion in hypertrophic cardiomyopathy is related to delayed contrast enhancement but not to systolic function: a PET and MRI study. *J Nucl Cardiol* 2006; 13:660–667.
26. Kramer CM, Reichek N, Ferrari VA, Theobald T, Dawson J, Axel L. Regional heterogeneity of function in hypertrophic cardiomyopathy. *Circulation* 1994;90:186–194.
27. Varnava AM, Elliott PM, Sharma S, McKenna WJ, Davies MJ. Hypertrophic cardiomyopathy: the interrelation of disarray, fibrosis, and small vessel disease. *Heart* 2000;84:476–482.
28. Knaapen P, van Dockum WG, Bondarenko O, Kok WE, Götte MJ, Boellaard R, Beek AM, Visser CA, van Rossum AC, Lammertsma AA, Visser FC. Delayed contrast enhancement and perfusable tissue index in hypertrophic cardiomyopathy: comparison between cardiac MRI and PET. *J Nucl Med* 2005;46:923–929.
29. Melacini P, Corbetti F, Calore C, Pescatore V, Smaniotto G, Pavei A, Bobbo F, Cacciavillani L, Iliceto S. Cardiovascular magnetic resonance signs of ischemia in hypertrophic cardiomyopathy. *Int J Cardiol* 2008;128:364–373.
30. Harris KM, Spirito P, Maron MS, Zenovich AG, Formisano F, Lesser JR, Mackey-Bojack S, Manning WJ, Udelson JE, Maron BJ. Prevalence, clinical profile, and significance of left ventricular remodeling in the end-stage phase of hypertrophic cardiomyopathy. *Circulation* 2006;114:216–225.
31. Popović ZB, Kwon DH, Mishra M, Buakhamsri A, Greenberg NL, Thamilarasan M, Flamm SD, Thomas JD, Lever HM, Desai MY. Association between regional ventricular function and myocardial fibrosis in hypertrophic cardiomyopathy assessed by speckle tracking echocardiography and delayed hyperenhancement magnetic resonance imaging. *J Am Soc Echocardiogr* 2008;21:1299–1305.
32. Thompson DS, Naqvi N, Juul SM, Swanton RH, Coltart DJ, Jenkins BS, Webb-Peploe MM. Effects of propranolol on myocardial oxygen consumption, substrate extraction, and haemodynamics in hypertrophic obstructive cardiomyopathy. *Br Heart J* 1980;44:488–498.
33. Choudhury L, Elliott P, Rimoldi O, Ryan M, Lammertsma AA, Boyd H, McKenna WJ, Camici PG. Transmural myocardial blood flow distribution in hypertrophic cardiomyopathy and effect of treatment. *Basic Res Cardiol* 1999;94:49–59.
34. Jensen CJ, Jochims M, Hunold P, Forsting M, Barkhausen J, Sabin GV, Bruder O, Schlosser T. Assessment of left ventricular function and mass in dual-source computed tomography coronary angiography: influence of beta-blockers on left ventricular function: Comparison to magnetic resonance imaging. *Eur J Radiol* 2010;74:484–491.